University of Groningen

PHOTOPHYSICAL AND PHOTOCHEMICAL MOLECULAR HOLE BURNING THEORY

DEVRIES, H; WIERSMA, DA; Vries, Harmen de

IMPORTANT NOTE: You are advised to consult the publisher's version (publisher's PDF) if you wish to cite from it. Please check the document version below.

Document Version
Publisher's PDF, also known as Version of record

Link to publication in University of Groningen/UMCG research database

Citation for published version (APA):
DEVRIES, H., WIERSMA, D. A., & Vries, H. D. (1980). PHOTOPHYSICAL AND PHOTOCHEMICAL MOLECULAR HOLE BURNING THEORY. Journal of Chemical Physics, 72(3), 1851-1863. DOI: 10.1063/1.439330

Photophysical and photochemical molecular hole burning theory

Harmen de Vries and Douwe A. Wiersma

Laboratory for Physical Chemistry, State University, Nijenborgh 16, 9747 AG Groningen, The Netherlands
(Received 7 August 1979; accepted 18 October 1979)

In this paper theories are given, describing photophysical and photochemical hole burning experiments on molecular mixed crystals at low temperature. Population saturation hole burning is treated for a two-level system where the lower level is the ground state. Hole burning due to a triplet state acting as a population bottle neck is also described by a steady-state density matrix theory. Connection is made with optical free induction decay. To obtain T_2 (the decay time of the off-diagonal elements of the density matrix), which is the main goal of these hole burning experiments, a linear extrapolation method is discussed. For photochemical hole burning a time-dependent density matrix treatment is given. Using this theory numerical simulations were performed of the experimental results obtained by Völker and co-workers for porphin in n-octane at low temperature. Good agreement with experiment is obtained. For this case extrapolation methods are discussed in order to obtain reliable T_2 values. A time-dependent kinetic theory is used to simulate the photochemical hole burning experiments on dimethyl-s-tetrazine in durene and s-tetrazine in benzene. This theory accounts for the recently revealed two-photon character of these photodissociations. It is shown that despite this complication the hole full width at half-maximum may still equal twice the homogeneous width of the S_o-S_1 transition.

I. INTRODUCTION

Quite recently we reported a study of the homogeneous width of an $S_0 - S_1$ transition in a molecular mixed crystal [dimethyl-s-tetrazine (DMST) in durene] at low temperature[1] using photochemical hole burning.[2,3] Such electronic transitions are mostly inhomogeneously broadened due to slight differences in the surroundings of the guest molecules. This indeed enables study of the homogeneous widths (dephasing times) by some kind of hole burning technique. Following this frequency domain experiment, these guest molecule $S_0 - S_1$ homogeneous widths were also studied with coherent transient methods: photon echoes on a nanosecond[4] and picosecond[5] timescale, and optical free induction decay (OFID).[6,7] A recent review on the study of homogeneous widths of electronic transitions in large molecules at low temperature is given in Ref. 8, where also preliminary results of the present work are reported. It turned out that at 1.5 K these widths are predominantly determined by the respective fluorescence lifetimes (τ_{f1}). This fact was utilized by us to determine the subnanosecond fluorescence lifetime of s-tetrazine (ST) in benzene at low temperature by photochemical hole burning.[9] When $T_2 = 2\tau_{f1}$[10] (T_2 being the decay time of the off-diagonal elements of the density matrix) and the excitation is monochromatic $(\Delta\nu_{exc} \ll 1/\pi T_2)$, in the low temperature solid the singlet S_1 state is prepared, as discussed in Ref. 10. Thus in the hole burning theories to be developed, we can consider simple energy level schemes (of singlet and triplet states).

There are several possibilities for the burning and observation of holes in inhomogeneously broadened absorption line shapes in order to study the homogeneous width of the transition under consideration. First we mention population saturation in a two-level system. This kind of hole burning is known in nuclear magnetic resonance since 1947.[11] In the optical domain it was first considered in gas laser studies,[12] while subsequently it was demonstrated in organic dye solutions at

room temperature.[13] A few years ago this kind of hole burning was used for the first time to study a solid[14]: Ruby was investigated using an amplitude-modulated cw ruby laser. However, the hole burning work on ruby[14,15] showed that a two-level model was insufficient to explain the experimental observations. This brings us to the hole burning caused by an intermediate level acting as a population bottle neck. In organic molecules often the lowest triplet state will serve as such, an early example being considered in Ref. 16. As the triplet lifetime can be very long (~1 s), in this kind of hole burning experiment it is possible to burn the hole first and probe it afterwards.[17] Theoretically this triplet bottle neck hole burning has not been considered in detail although it is contained in our molecular OFID theory.[18] The relation between theoretical hole burning and OFID results is pointed out in Secs. II and III below. The types of hole burning just mentioned are photophysical in nature. Finally we have the case of photochemical hole burning, where the irradiated molecules undergo, for example, photodissociation. Permanent holes can then be burnt from which homogeneous widths may be obtained, as demonstrated in Refs. 1 and 9. It should be noted that permanent holes may also be burnt, when irradiation causes a physical change in the molecular environment (see Sec. IV). This is another type of photophysical hole burning.

As already mentioned, two-level saturation hole burning is known for a long time in gas phase studies.[12] These experiments have been described theoretically by several authors, using the density matrix, or kinetically. It was always assumed that both levels could decay spontaneously to other levels. However, for the $S_0 - S_1$ transitions of interest to us, the lower level is the ground state. In order to obtain a coherent treatment of the different types of hole burning, it seemed appropriate to us, to first discuss two-level saturation hole burning where the lower level is the ground state. This is done in Sec. II. In Sec. III the theory is extended, to include triplet population bottle neck hole burning. The
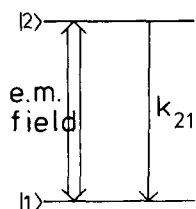
FIG. 1. Two-level model system, subjected to saturating and probe beams. Level $|2\rangle$ decays by spontaneous emission (rate k_{21}) to the ground state $|1\rangle$.

work reported here was primarily started to obtain a *microscopic theory* for irreversible photochemical hole burning. Here irreversible means that the photochemical transformation does not proceed in the reverse direction during the hole burning experiment. As a consequence one cannot consider a closed pumping cycle and time-dependent solutions of the equations of motion have to be obtained (Sec. IV). To this end we have applied the Laplace transformation technique, which in this case often will require the solution of equations of degree 4 or higher. Studying a specific example of irreversible photochemical hole burning one will have to perform these solutions numerically. Despite this fact the theoretical method described in Secs. IV and V is applicable to any hole burning experiment of that kind (taking into account the particular pumping cycle under consideration). In fact, the methodology used in the present paper will also be applicable in the study of reversible (in the sense just mentioned) photochemical or photophysical hole burning. To determine T_2 of the $S_0 - S_1$ transition one then may choose, for the hole burning study to be performed, different time scales relative to the rate of the reverse process. The design of the experiment has to be adapted accordingly (probing simultaneous with or after burning). Depending on which way was chosen to solve the problem, steady-state or time-dependent theories have to be used, similar to the ones given below. For example, already the participation of the intermediate triplet state in the pumping cycle discussed in Sec. III may be seen as a reversible loss from the $S_0 - S_1$ level system. In this context we would like to refer to Ref. 10, Sec. IV D, where the influence of the triplet state upon the time and detuning dependence of the S_1 population is discussed.

When the relevant kinetic and other parameters of the specific molecular system are all known, one may possibly obtain a reliable value of T_2 from a comparison of the experimental with the numerically simulated dependences of the hole width against the burning power and the burning time. An example of irreversible photochemical hole burning is the study of porphin in n-octane,[19] where the process was described in a phenomenological way. It seemed of interest to simulate the experimental results using our microscopic theory. Also the triplet state should be taken into consideration here, and we applied the density matrix theory of Sec. IV. This is done in Sec. V A. It turns out that here T_2 can be obtained by a linear extrapolation method as a function of the burning power. Other examples of irreversible photochemical hole burning are the studies of DMST in durene and ST in benzene, already mentioned above. Still little is known about the precise photodissociative chemical reactions taking place in these cases.

Recently more physical insight in these processes was obtained (two-photon character).[20-22] This was taken into account in our simulations of these hole burning experiments, where a time-dependent kinetic theory was used. This can be found in Sec. V B and V C.

It should be noted that we will leave energy transfer (spectral diffusion) processes out of consideration.

II. TWO-LEVEL SATURATION HOLE BURNING

A. Population hole burning

In this type of experiment the sample is radiated by two beams simultaneously: the saturating one and a non-saturating probe beam. Theories have been developed for gaseous samples, where the transitions under study are inhomogeneously broadened by the Doppler effect, implying the importance of the relative direction of the two beams. A recent review on this saturation spectroscopy can be found in Ref. 23. In the literature on this subject mostly pseudo-two-level systems are considered, where both levels can decay to other levels (see, for example, Ref. 24).

In the study of organic dye solutions, suitable as saturable absorbers in solid state (Nd glass, ruby) lasers, the power saturation hole burning was also demonstrated.[13] This observation was described theoretically with a kinetic two-level model including the effect of spectral diffusion.[25,26] We note once again that this latter effect will not be considered in the present work.

In this paper we consider molecular mixed crystal samples, especially the $S_0 - S_1$ transition of the guest molecules. As the microscopic environments of these molecules are slightly different, also in this case the transitions of interest are inhomogeneously broadened. This broadening may differ for different transitions in the system studied,[9,27,28] in contrast to the Doppler broadening in gases. We therefore want to note here that in mixed crystals the applicability of saturation experiments on coupled transitions will at least be severely limited, compared to the gasphase.[23]

First we now want to consider the two-level system of Fig. 1, where the only decay process is the $|1\rangle \leftarrow |2\rangle$ spontaneous emission. Suppose we have an ensemble of such two-level atoms embedded in a host matrix. A monochromatic saturating beam of light is directed to this sample, with its frequency tuned to the center of the inhomogeneously broadened $|1\rangle - |2\rangle$ transition. The saturated absorption line shape is probed by a nonsaturating monochromatic beam, traveling in the opposite direction. We will derive a formula for the line shape as detected by the probe beam. Applying the rotating wave approximation we write down the following set of equations of motion for the density matrix elements:

$$\dot{\tilde{\rho}}_{12} = \left(i\Delta - \frac{1}{T_2}\right)\tilde{\rho}_{12} + \tfrac{1}{2} i\chi(\rho_{22} - \rho_{11}) \tag{1}$$

$$\dot{\rho}_{11} = k_{21}\rho_{22} + \tfrac{1}{2} i\chi(\tilde{\rho}_{21} - \tilde{\rho}_{12}) \tag{2}$$

$$\dot{\rho}_{22} = -k_{21}\rho_{22} + \tfrac{1}{2} i\chi(\tilde{\rho}_{12} - \tilde{\rho}_{21}) \tag{3}$$

$$\rho_{11} + \rho_{22} = 1 . \tag{4}$$

Here $\Delta = \omega_s - \bar{\omega}_0$ gives the detuning between the saturating beam angular frequency ω_s and the homogeneous line center $\bar{\omega}_0$. $\bar{p}_{12} = \rho_{12} \exp[-i(\omega_s t - kz)]$[29] for a saturating beam propagating in the z direction (wave vector k). $\chi = \mu_{12} E_0/\hbar$ is the on-resonance Rabi frequency, where E_0 is the absolute value of the saturating electric field amplitude $\mathbf{E}_0$ and μ_{12} is the value of the component along $\mathbf{E}_0$ of the transition dipole moment μ. T_2 is the phenomenologically added decay time of $\bar{p}_{12}$. From Eqs. (2)–(4) one can easily derive an equation of motion for the quantity $\rho_{11} - \rho_{22}$, giving the population difference. As the decay time appearing in this equation is known as the longitudinal relaxation time T_1,[30] we have $T_1 = 1/k_{21}$.

It is important to note that the interaction with the probe field is not included in these equations (see below). As we want to find here the saturated population difference, we determine the steady state solution for $\rho_{11} - \rho_{22}$:

$$\rho_{11} - \rho_{22} = \frac{\Delta^2 + \frac{1}{T_2^2}}{\Delta^2 + \frac{1}{T_2^2} + \frac{\chi^2 T_1}{T_2}} \cdot \tag{5}$$

As we consider a Gaussian inhomogeneously broadened transition (with an FWHM of $\Delta\omega_G$), expression (5) has to be multiplied by this line shape function:

$$W(\bar{\omega}_0) = \exp\left[-\left(\frac{2\sqrt{\ln 2}\,(\bar{\omega}_0 - \omega_s)}{\Delta\omega_G}\right)^2\right], \tag{6}$$

where it is assumed that ω_s is tuned to the inhomogeneous line center. In order to obtain a formula for the absorption coefficient α for the probe beam as a function of the probe frequency ω_p, the expression for $\rho_{11} - \rho_{22}$ has to be convoluted with the Lorentzian homogeneous line shape function[31]:

$$\alpha(:) \frac{1}{\pi T_2} \int_0^\infty \frac{\Delta^2 + \frac{1}{T_2^2}}{\Delta^2 + \frac{1}{T_2^2} + \frac{\chi^2 T_1}{T_2}}\, W(\bar{\omega}_0)\, \frac{1}{(\omega_p - \bar{\omega}_0)^2 + \frac{1}{T_2^2}}\, d\bar{\omega}_0 . \tag{7}$$

This agrees with expression (3) of Ref. 32, derived for the case where both levels can decay to other levels.[33] We assume the inhomogeneous width to be much broader than the part of the line pumped by the saturating laser. Therefore the factor W can be taken outside the integral and evaluated for $\bar{\omega}_0 = \omega_p$. The remaining integral can be solved by contour integration, yielding:

$$\alpha(:) W(\omega_p)\left[1 - \frac{\chi^2 T_1}{\sqrt{1 + \chi^2 T_1 T_2}} \frac{\frac{1}{T_2}(1 + \sqrt{1 + \chi^2 T_1 T_2})}{\Delta_p^2 + \frac{1}{T_2^2}(1 + \sqrt{1 + \chi^2 T_1 T_2})^2}\right], \tag{8}$$

which is identical to the result of Sargent and Toschek[32] [their Eq. (17)]. Δ_p is defined as $\omega_p - \omega_s$, the detuning between probe and saturating frequencies. Clearly the first factor of expression (8) gives the unsaturated absorption coefficient, while the second factor gives the Lorentzian hole shape.

We assume the sample to be optically thin, so the saturating and probe beam intensities are essentially constant across it. Then formula (8) describes directly the line shape as observed in an absorption or excitation experiment.

For the FWHM of the observed hole one obtains from (8):

$$2\pi\Delta\nu^h = \Delta\omega^h = \frac{2}{T_2}(1 + \sqrt{1 + \chi^2 T_1 T_2}) \tag{9}$$

a result, known in saturation spectroscopy for several years already.[23] One can make the following comments here. First, extrapolating the measured hole width to zero saturating power, the homogeneous width of the transition is obtained:

$$\lim_{\chi^2 \to 0} \Delta\nu^h = \frac{2}{\pi T_2} = 2\Delta\nu^{HOM} . \tag{10}$$

Second, it is interesting to note the connection between hole burning and optical free induction decay (OFID) spectroscopy for the two-level system[29]:

$$\Delta\omega^h = \frac{2}{\tau_{OFID}} , \tag{11}$$

where τ_{OFID} is the $1/e$ decay time of the OFID beat amplitude. For the depth of the hole relative to the unsaturated absorption value, we obtain from (8):

$$D = \frac{\chi^2 T_1 T_2}{\sqrt{1 + \chi^2 T_1 T_2} + 1 + \chi^2 T_1 T_2} . \tag{12}$$

B. Possible complications

Thus far we have treated the population hole as burned by a saturating beam and probed by an independent nonsaturating beam. The closely related problem of hole burning by stimulated emission in the population of the upper level of a maser medium was discussed by Bennett.[12] In this paper for the first time population hole burning in the optical domain was considered. However, the process taking place in the sample interacting simultaneously with the saturating and probe beams is, in principle, not completely described by the "Bennett hole burning." A complete description is obtained by including the interaction with the probe field in the equations of motion for the density matrix elements.[34-36] In Refs. 32 and 33 the problem is solved using a high-intensity laser theory. These theories result in expressions for the probe absorption coefficient, consisting of two contributions. The first part is the population hole burning result obtained above. The second contribution to α is the so called coherent part.[32] This second part gives hole shapes which differ for opposing and unidirectional beams, and this part becomes increasingly important as the saturating power is increased. For opposing beams the coherent contribution is the largest for the case where both energy levels have identical decay rates, but it vanishes when these rates are very different.[34,35] In the present paper we are interested in the situation where one of the two states coupled by the radiation fields is the ground state. Moreover, we assume opposing saturating and probe beams. Therefore we can further leave the coherent contribution to α out of consideration.

To obtain reliable T_2 values from hole burning measurements, one would require $\Delta\nu_s, \Delta\nu_p < \Delta\nu^{HOM}$, where

$\Delta \nu_s$ and $\Delta \nu_p$ are the bandwidths of the saturating and probe beams, respectively. When this inequality holds one has to be concerned about the Weisskopf–Heitler effect[37,38]: when a two-level system as that of Fig. 1, where $\Delta \nu^{HOM} = 1/\pi T_2 = 1/2\pi T_1$, is excited by monochromatic light, the scattered radiation has the same bandwidth as the exciting light instead of the (greater) width $\Delta \nu^{HOM}$. This effect was experimentally demonstrated by Gibbs and Venkatesan.[39] In this elastic scattering process no real population of level $|2\rangle$ takes place, which might make a population hole burning experiment impossible. However, for high power monochromatic excitation the elastically scattered intensity becomes negligible and the scattering process is predominantly inelastic[40,41]: level $|2\rangle$ is populated. As in a saturation hole burning experiment one would necessarily use excitation powers, such that $\chi^2 T_2^2/2 \gtrsim 1$,[40] this experiment is *in principle* very well possible.

Having discussed the two-level population saturation hole burning and some possible complications, we now turn to the molecular level scheme where an electronic triplet state is lying in between the two singlet levels coupled by the radiation fields.

III. POPULATION BOTTLE NECK HOLE BURNING

A hole burning experiment of this kind is possible when in addition to the (inhomogeneously broadened) optical transition a long living state participates in the pumping cycle, acting as a population bottle neck. Such long living levels are very common: for example, the lowest triplet state, lying in between the lowest two singlet states in organic molecules, and ground-state hyperfine levels in atoms, ions, and molecular radicals.[42,43] The bottle neck effect of these levels becomes very clear where they cause transient fluorescence signals.[6,10,44] Also in OFID experiments these long living levels are important,[6,10,18,45,46] while in dye lasers they cause the lasing medium to be pumped rapidly across the excitation point.

An early example of spectral hole burning in the condensed phase probably caused by population build up in a triplet state, is given by Spaeth and Sooy[16] in a study of saturable absorbers for ruby lasers. Population hole burning experiments where the bottle neck is formed by ground state hyperfine levels were performed on the $^1D_2 - {}^3H_4$ transition of Pr^{3+}: LaF_3.[47–49] A similar effect has been studied for a gas phase sample of Na atoms.[50] Hole burning due to triplet state population was observed for a frozen solution of chlorophyll a in ether.[51] Recently triplet state population hole burning was reported for F_3^* color centers in NaF[52] and for zinc porphin in n-octane.[17] Also in the photochemical hole burning work of Völker *et al.*[19,53] for porphin in n-octane the triplet state population should be considered, as here the $T - S_1$ intersystem crossing (ISC) quantum yield is 0.9 (see Sec. V A).

In the literature quoted so far a formula relating the hole width to the population build up in the bottle neck level is very rare. In Refs. 54 and 55 photochemical hole burning, where the induced molecular transformation exhibits reversibility during the experiment, is studied (see Sec. IV) for some large organic molecules
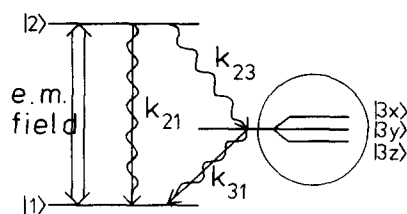

FIG. 2. Molecular model system, subjected to saturating and probe beams. Straight and wavy arrows indicate radiative and radiationless transitions, respectively. The part within the circle has a greatly magnified ($\sim 10^4$) energy scale. $|3x\rangle$, $|3y\rangle$, and $|3z\rangle$ denote the triplet spin sublevels.

in low temperature matrices. Kinetic theories were developed in these studies including the intermediate triplet states. Only in Ref. 55 a hole width formula was given for triplet state population hole burning.

We now consider the molecular level scheme of Fig. 2. Level $|1\rangle$ is the singlet ground state S_0, $|2\rangle$ is the first excited singlet state S_1 and $|3\rangle$ is the lowest triplet state T. Compared to Fig. 1, level $|2\rangle$ now has two additional decay channels: $S_0 - S_1$ internal conversion and $T - S_1$ ISC (rate k_{23}). k_{21} denotes the total $S_0 - S_1$ decay rate (radiative plus radiationless), while the same holds for k_{31} with respect to the $S_0 - T$ decay. As we are considering in this paper low temperature molecular mixed crystals, this level scheme is considered to provide a good description of the process of interest.[10] Again a monochromatic saturating beam is directed to the sample, with ω_s tuned to the center of the inhomogeneously broadened $|1\rangle - |2\rangle$ transition, while a nonsaturating monochromatic probe beam is coming from the opposite direction. The derivation of the saturated absorption line shape, as detected by the probe, proceeds in a similar way as for the two-level case of Sec. II. The equations of motion for the density matrix elements for the three-level system are:

$$\mathring{\rho}_{11} = k_{21}\rho_{22} + k_{31}\rho_{33} + \tfrac{1}{2} i\chi (\bar{\rho}_{21} - \bar{\rho}_{12}) \tag{13}$$

$$\mathring{\rho}_{22} = -K_2\rho_{22} + \tfrac{1}{2} i\chi (\bar{\rho}_{12} - \bar{\rho}_{21}) \tag{14}$$

$$\mathring{\rho}_{12} = \left(i\Delta - \frac{1}{T_2}\right)\bar{\rho}_{12} + \tfrac{1}{2} i\chi (\rho_{22} - \rho_{11}) \tag{15}$$

$$\dot{\rho}_{33} = k_{23}\rho_{22} - k_{31}\rho_{33} \tag{16}$$

$$\rho_{11} + \rho_{22} + \rho_{33} = 1 . \tag{17}$$

K_2 is the total decay constant of level $|2\rangle$: $K_2 = k_{21} + k_{23}$. The other quantities have been defined earlier. The steady state solution of Eqs. (13)–(17) yields for the $|1\rangle - |2\rangle$ population difference

$$\rho_{11} - \rho_{22} = \frac{\Delta^2 + \dfrac{1}{T_2^2}}{\Delta^2 + \dfrac{1}{T_2^2} + \hat{K}^2} . \tag{18}$$

Here $\hat{K}^2$ is defined according to $\hat{K}^2 = \chi^2(2 + A)/2T_2K_2$, where $A = k_{23}/k_{31}$.[18] The term $\hat{K}^2$ gives rise to the combined effects of power saturation (Sec. II) and triplet bottle neck hole burning. Taking into account the three spin-sublevels $|3x\rangle$, $|3y\rangle$, and $|3z\rangle$ again yields Eq. (18), where now $A = \sum_i (k_{23}^i/k_{31}^i)$. In a similar manner as for the two-level system we obtain instead of Eq. (8):

$$\alpha(:)W(\omega_p)\left[1 - \frac{\hat{K}^2}{\sqrt{1+\hat{K}^2T_2^2}}\frac{1+\sqrt{1+\hat{K}^2T_2^2}}{\Delta_p^2 + \frac{1}{T_2^2}(1+\sqrt{1+\hat{K}^2T_2^2})^2}\right]. \quad (19)$$

Again the second factor gives the Lorentzian hole shape. For an optically thin sample we obtain for the observed hole FWHM from (19):

$$2\pi\Delta\nu^h = \Delta\omega^h = \frac{2}{T_2}(1 + \sqrt{1+\hat{K}^2T_2^2}) . \quad (20)$$

In Ref. 55 a similar formula is obtained. However, there the second term under the square root sign contains the factor $(k_{23}+k_{31})/k_{31}K_2$ instead of the factor $(2k_{31}+k_{23})/k_{31}K_2$ in our case. The homogeneous width of the $|1\rangle - |2\rangle$ transition again can be obtained by extrapolating the measured hole width to zero saturating power [Eq. (10)]. Also for the molecular model system of Fig. 2 we obtain for the connection between hole burning and OFID[18] spectroscopy the relation (11): $\Delta\omega^h = 2/\tau_{\text{OFID}}$. Thus as in the case of molecular OFID[10,18] from the extrapolation to zero power one can obtain the $S_0 - S_1$ transition dipole moment *or* the ISC rate k_{23}, depending on which of the two quantities was known already. For the relative hole depth we now obtain, instead of (12):

$$D = \frac{\hat{K}^2T_2^2}{\sqrt{1+\hat{K}^2T_2^2}+1+\hat{K}^2T_2^2} . \quad (21)$$

The bottle neck population may give rise to substantial hole broadening already when the "pure" power broadening is not yet operative. An example where the different kinds of hole burning are compared, is given in Sec. V A. Note that for $K_2 = 1/T_1$ and $A = 0$ the three- (or five-) level formulas for $\alpha(\Delta_p)$, $\Delta\omega^h$, and D reduce to the corresponding two-level ones. It should also be noted that, in a similar way as for OFID,[6] a linear extrapolation to zero power may be obtained, using the relation [which follows from (20)]:

$$\pi T_2(\Delta\nu^h)^2 - 2(\Delta\nu^h) = \frac{\chi^2(2+A)}{2\pi K_2} . \quad (22)$$

Experimentally $\Delta\nu^h$ is determined as a function of the saturating laser power, which is proportional to E_0^2. For different chosen values of T_2 the left hand side of Eq. (22) is plotted as a function of E_0^2 (least squares fit to the experimental points). When this straight line passes the origin, the correct value of T_2 is obtained. The slope of this line will give one of the quantities μ_{12} or k_{23}, when the other one is known from other experiments.

Triplet-bottle neck hole burning may thus occur for a laser power which for the corresponding two-level system would not have been saturating (Sec. V A). Therefore, as one still would require $\Delta\nu_s$, $\Delta\nu_p < \Delta\nu^{\text{HOM}}$, the Weisskopf-Heitler effect should also be considered for this case (compare Sec. II). Note that we consider in this paper the case $T_2 = 2\tau_{t1}$[10]$(\tau_{t1} = 1/K_2)$. As already mentioned in the Introduction the molecular level structure in the condensed phase is very well-described by the simple picture of singlet and triplet levels of Fig. 2. Compared to the case of Fig. 1 we have from level $|2\rangle$ not only elastic (isoenergetic) light scattering but also isoenergetically radiationless transitions. While level $|2\rangle$ is still being excited, the internal conversion to S_0^*

and the ISC to T^* already do take place. S_0^* and T^* are the isoenergetic (with S_1) vibronic levels of S_0 and T, and are not shown in Fig. 2. In the condensed phase S_0^* and T^* immediately ($\sim$ps[56]) decay by vibrational relaxation to their respective purely electronic levels. Thus in this case for low power with $\Delta\nu_s < \Delta\nu^{\text{HOM}}$ we obtain real population of the T state $|3\rangle$ and we may apply the bottle neck hole burning theory just given.

Finally it is interesting to note that in the case of a homogeneously broadened $S_0 - S_1$ transition in the solid phase (azulene in naphthalene), where S_1 predominantly decays by $S_0 \leftarrow S_1$ internal conversion, the Weisskopf-Heitler effect has recently been observed.[57]

IV. PHOTOCHEMICAL HOLE BURNING

In the previous sections we discussed population (two-level saturation and bottle neck) hole burning where the molecular structure was not affected by the saturating light. In this section, however, we consider the case where the molecules of interest undergo photochemical transformation, photodissociation, or possibly photoionization. Some of these processes will exhibit reversibility while others will be irreversible. Therefore in these cases, using a monochromatic laser beam, one can burn holes in an inhomogeneously broadened absorption line, which may be long living (compared to the molecular level decay rates) or permanent. Thus in such experiments it is possible to first burn a hole and subsequently probe it by a scanning laser of weak intensity, which causes negligible burning. In these photochemical hole burning experiments the coherent contribution to α as discussed in Sec. II will in principle be absent. As the molecules, disappearing from the burning frequency, no longer contribute with their homogeneous width to the absorption line of interest, it will be clear that also photochemical hole burning may be used to obtain the transverse relaxation time T_2 for the transition studied.

The first observations of stable holes burnt in inhomogeneously broadened molecular transitions were reported in 1974 by Kharlamov, Personov, and Bykovskaya[2] and by Gorokhovski, Kaarli, and Rebane.[3] In Ref. 2 perylene and 9-aminoacridine in ethanol at 4.2 K were studied. From the burnt holes $S_0 - S_1$ homogeneous widths of ~ 0.4 cm^{-1} were estimated. In Ref. 3 holes were burnt in the 0–0 transition line of a solid solution of H_2–phthalocyanine in n-octane at 4.2 K. The holes had an instrument limited width of ~ 0.2 cm^{-1}. Photochemical hole burning for an $S_0 - S_1$ transition in a molecular mixed crystal using a single-frequency cw dye laser was reported by the present authors.[1] For DMST in durene at 2 K a hole width (recorded in the excitation spectrum) was obtained of 120 MHz (0.004 cm^{-1}). Gorokhovski, Kaarli, and Rebane later repeated their experiment using a narrow line ruby laser and obtained a homogeneous width of $\simeq 0.03$ cm^{-1} for the transition studied.[58] Photochemical hole burning in the $S_0 - S_1$ transition of free base porphin in n-octane at 4.2 K was subsequently reported by Völker and van der Waals,[59] where pulsed and cw dye lasers were used. Results of continued studies by authors already mentioned are presented in Refs. 9,19,53,55,60–62. Photochemical hole
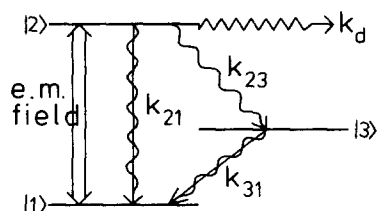
FIG. 3. Kinetic scheme used to describe one-photon photo-chemical hole burning upon $S_1 \leftarrow S_0$ excitation. The loss of population from the system due to the phototransformation is denoted by k_d.

burning studies performed on different systems can be found in Refs. 52, 63, 64.

It was recently also noted that a narrow band excitation source may remove molecules from their original absorption frequency within the inhomogeneous line by a *physical* change in the molecular environment.[65,66] It was suggested that some stable holes reported earlier[2,54] would also be due to such a process. When this photo-physical hole burning is irreversible (during burning), a theory will apply to it like that given below for photochemical hole burning. Such a photophysical hole burning has also been observed in the optical spectra of trapped electrons in organic glasses.[67] Recently a similar photophysical hole burning effect was reported in the infrared for a vibrational transition of 1, 2-difluoroethane in an Ar matrix at low temperature.[68]

It seems interesting to note here that the applicability of photochemical hole burning in optical memory systems was recently patented.[69]

Theoretical descriptions of photochemical (photophysical) hole burning have been given in Refs. 54 and 55. These were steady-state kinetic theories for reversible cases where the photo process occurs simultaneously with the reverse process. In Ref. 19 the irreversible (in a sense just mentioned) process is described in a phenomenological way. We would prefer a molecular theory for the irreversible process, where the interaction with the radiation field is treated from first principles. From such a theory it should follow which extrapolation method is the best to obtain $T_2(\Delta v^h$ as a function of the burning power or the burning time).

As in Secs. II and III, one would like to start with the equations of motion for the density matrix elements. In principle the photoreaction upon $S_1 \leftarrow S_0$ excitation may occur from different states: a vibronic S_0 level, the electronic S_1 state or a vibronic T level. These possibilities lead to different kinetic schemes. For our purposes, however, the final theoretical result is independent of the particular scheme chosen. The reason for this is that the burning times are considered to be much longer than the inverse of the decay rates in the system, while for all the schemes we would take the same value for the quantum yield from S_1 ($\emptyset$) of the photoreaction. We therefore choose the most simple kinetic scheme applicable (Fig. 3), where the reaction takes place directly from S_1. We will consider only one triplet spin-sublevel $|3\rangle$. The inclusion of three $|3i\rangle$ levels, however, is straightforward.

Suppose the burning laser (angular frequency ω_B) is tuned to the center of the inhomogeneous line. The beam is directed to the sample at time $t = 0$ and shut off at $t = t_{off}$. We have to find time-dependent solutions for the following set of density matrix equations of motion

$$\dot{\rho}_{11} = k_{21}\rho_{22} + k_{31}\rho_{33} + \tfrac{1}{2} i\chi(\tilde{\rho}_{21} - \tilde{\rho}_{12}) \quad (23)$$

$$\dot{\rho}_{22} = -K_2\rho_{22} + \tfrac{1}{2} i\chi(\tilde{\rho}_{12} - \tilde{\rho}_{21}) \quad (24)$$

$$\dot{\rho}_{33} = k_{23}\rho_{22} - k_{31}\rho_{33} \quad (25)$$

$$\dot{\tilde{\rho}}_{12} = (-\Gamma + i\Delta)\tilde{\rho}_{12} + \tfrac{1}{2} i\chi(\rho_{22} - \rho_{11}) \quad (26)$$

$$\dot{\tilde{\rho}}_{21} = (-\Gamma - i\Delta)\tilde{\rho}_{21} - \tfrac{1}{2} i\chi(\rho_{22} - \rho_{11}) \ . \quad (27)$$

Here $\chi = \mu_{12} E_0/\hbar$ where E_0 is the absolute value of the burning electric field amplitude $\mathbf{E}_0$. $\Delta = \omega_B - \bar{\omega}_0$ is the detuning between the burning laser and the homogeneous line center $\bar{\omega}_0$. $K_2 = k_{21} + k_{23} + k_d$ is the total decay rate from level $|2\rangle$, while $\Gamma = 1/T_2$. The time-dependent solutions of these equations are obtained using the Laplace transformation technique, as shown in detail in the Appendix.

When the burning laser is suddenly shut off, the relative level populations are $\rho_{11}(t_{off}, \Delta), \rho_{22}(t_{off}, \Delta)$, and $\rho_{33}(t_{off}, \Delta)$. After the decay of the excited states, the ground state population as a function of the detuning Δ is proportional to:

$$\rho_{11}(\Delta) = \{\rho_{11}(t_{off}, \Delta) + (1 - \emptyset)\rho_{22}(t_{off}, \Delta) + \rho_{33}(t_{off}, \Delta)\} \ , \quad (28)$$

where it is recalled that $\emptyset$ was the quantum yield from S_1 for the photoreaction. In addition to the remarks made in the beginning of Sec. II on different inhomogeneous distributions in different transitions, it is interesting to note that here the population of level $|3\rangle$ is labeled according to their $|1\rangle - |2\rangle$ transition frequencies (Δ).

The hole in the ground state population as given by Eq. (28) will be subsequently probed. We assume the hole probing not to cause significant phototransformation, power saturation or triplet population build up. One then has to use a probe laser of low intensity, scanning fast enough through the frequency region of interest. Otherwise extrapolation to zero probe intensity will be necessary.[17,68] The Gaussian inhomogeneous lineshape has still to be taken into account:

$$W = \exp\left[-\left(\frac{2\sqrt{\ln 2}\Delta}{\Delta\omega_G}\right)^2\right] \ , \quad (29)$$

where the burning frequency ω_B is tuned to the line center. For the probe absorption coefficient we now obtain:

$$\alpha(:)\frac{1}{\pi T_2} \int_0^\infty \rho_{11}(\Delta)W \frac{1}{(\omega_p - \bar{\omega}_0)^2 + \frac{1}{T_2^2}} \, d\bar{\omega}_0 \ , \quad (30)$$

where ω_p is the probe angular frequency. Again assuming optically thin samples, expression (30) directly gives the hole shape as observed in an absorption or excitation experiment.

V. APPLICATIONS

A. Porphin in *n*-octane

In this case the two porphin inner hydrogens may occupy two positions. In the low temperature matrix these

two forms may be transformed into one another using narrowband irradiation.[59] It was shown to be a one-photon process. Although Völker and van der Waals discuss the phototransformation following $T - S_1$ ISC,[59] we can use the model system of Fig. 3, as outlined in the previous section. Using the theory given above we performed numerical simulations of porphin hole burning experiments. We tried to reproduce the results obtained by Völker et al.[19] experimentally and also considered some extrapolation methods in order to obtain T_2 from such experiments.

Now the simulation program will be shortly discussed. First the detuning of $\bar{\nu}_0$ relative to ν_B (these are the frequencies corresponding to their respective angular frequencies) is varied from 0 to plus and minus 500 MHz with a resolution of 2 MHz. For each detuning value the roots of Eq. (A9) were calculated as described in the Appendix. Depending on all roots being real, expressions (A11), (A14), and (A17) were calculated or the corresponding expressions for the complex case. For a certain value of the probe frequency ν_p the summation corresponding to Eq. (30) was carried out for $\nu_B - \bar{\nu}_0$ running from -500 to $+500$ MHz (resolution 2 MHz). This gives the probe absorption coefficient $\alpha(\nu_p)$. To obtain the observed hole shape, ν_p was varied over a sufficiently large region (mostly from $-240 + \nu_B$ MHz to $+240 + \nu_B$ MHz) with a resolution of 2 MHz. Finally plots were made of the ground state population hole [Eq. (28)] as well as of the hole in $\alpha(\nu_p)$. It should be noted here that the inhomogeneous line shape was included in the numerical integration (30). Thus this line shape was taken into account more exactly than in the analytical formulas (8) and (19).

For the kinetic parameters we chose the following values: $k_{31} = 100$ s^{-1} [69] and $K_2 = 5.94 \times 10^7$ s^{-1}, corresponding to $\tau_{f1} = 16.84$ ns.[19] As $\emptyset$ was taken to be 0.01[70] we get $k_d = 5.94 \times 10^5$ s^{-1}. Further $k_{21} = 5.88 \times 10^6$ s^{-1} and $k_{23} = 5.292 \times 10^7$ s^{-1} ($|3\rangle \rightarrow |2\rangle$ ISC yield $\sim 90\%$[71]), while $T_2 = 2\tau_{f1}$ (Ref. 10, footnote 21) as we consider the low temperature limit where additional dephasing mechanisms are absent. It should be noted that in the simulations we use monochromatic beams.

We like to obtain results which may be compared with the experimental ones of Völker et al.[19], as far as this is permitted by the precision of the latter report. They used a burning power density at the sample of 0.5 mW/cm². This yields $E_0^2 = 3.67 \times 10^3$ V²/m² when no local field correction is applied. We take $\mu_{12}^2 = 0.21 \times 10^{-60}$ C²m²,[18] where μ is assumed to be parallel to E_0. This results in $\chi^2 = 6.93 \times 10^{10}$ s^{-2}. However, using this χ^2 value we obtain hole widths (in α) of 49.3 to 108.6 MHz when t_{off} is varied from 1 to 8 s. This is an increase substantially larger than the 30% quoted in Ref. 19. We get this $\sim 30\%$ increase for $\chi^2 = 2.97 \times 10^9$ s^{-2}. Taking into account the local field correction, the assumptions made in calculating μ^2 and the polarization of E_0 relative to μ, this value of χ^2 might correspond to the power density of 0.5 mW/cm².

Now we will present the results of the simulations. In Fig. 4 we show an example of a ground state population hole [$\rho_{11}(\Delta)$] and the corresponding hole in α as calcu-
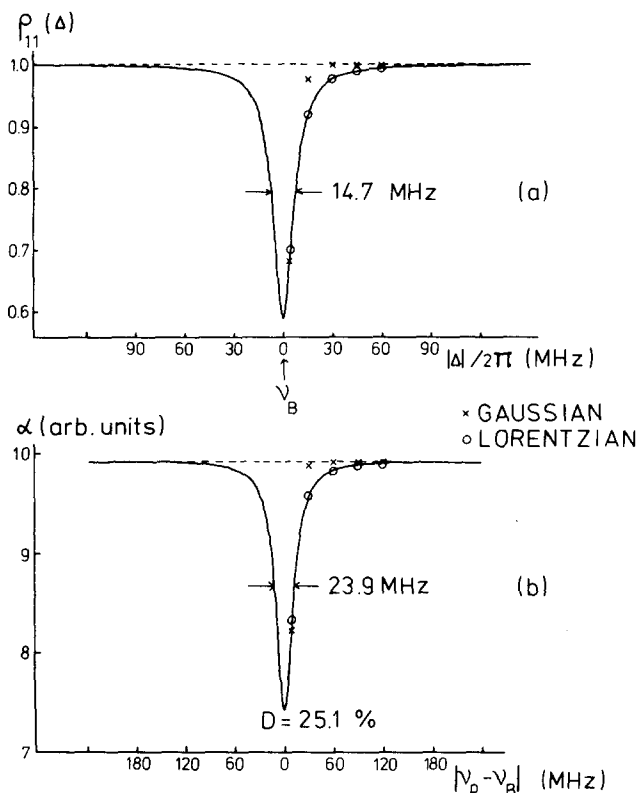

FIG. 4. Porphin in n-octane at low temperature ($T_2 = 2\tau_{f1}$). Computer calculated holes in $\rho_{11}(\Delta)$ (a) and in the probe absorption coefficient α (b). These holes are obtained with a burning time $t_{off} = 1$ s and a burning laser power $\chi^2 = 5.94 \times 10^9$ s^{-2}.

lated by the computer program just discussed. As indicated both hole shapes are Lorentzian. Note that for the closed three-level system (Sec. III) the analytical formulas (18) and (19) also exhibit Lorentzian holes. Further note that the sum of the $\rho_{11}(\Delta)$ – hole width and the homogeneous width $1/\pi T_2 = 9.45$ MHz just equals the width of the hole in α (within the limits of accuracy), as it should be for Lorentzians.

For $\chi^2 = 2.97 \times 10^9$ s^{-2} the holes in α were calculated as a function of the burning time t_{off}. The results are shown in Fig. 5. In the region 1 to 8 s, $\Delta\nu^h$ increases linearly with t_{off} for both burning powers. For $\chi^2 = 2.97 \times 10^9$ s^{-2} this increase is about 30%. These findings agree with the experimental ones.[19]

Next, holes in α were calculated as a function of the burning power (χ^2). We also calculated $\Delta\nu^h$ as a function of the burning power for the corresponding closed two-level and three-level systems, using Eqs. (9) and (20), respectively. Here for k_{21}, k_{23}, and k_{31} the same values were taken as in the porphin calculations. The only change for the photochemical case compared to the closed three-level system is the addition of the decay rate k_d. These burning (saturating) power dependent results are depicted in Fig. 6. This figure shows a beautiful comparison of the different types of hole burning as discussed in Secs. II–IV. In the χ^2 range considered, the power term in Eq. (9) remains unimportant compared to 1 (curve a). However, for the closed three-level case (curve b) the triplet bottle neck already
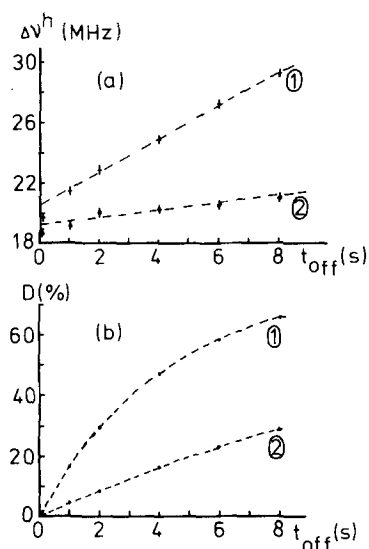
FIG. 5. Porphin in n-octane at low temperature $(T_2 = 2\tau_{t1})$. FWHM $\Delta\nu^h$ (a) and relative depth D (b) of holes in the probe absorption coefficient α, calculated as a function of the burning time t_{off}. These calculations were performed for $\chi^2 = 2.97 \times 10^9$ s^{-2} (1) and $\chi^2 = 5.94 \times 10^8$ s^{-2} (2). The accuracy in the values of $\Delta\nu^h$ is ± 0.3 MHz and in the values of $D \pm 0.1\%$.

causes considerable hole broadening. Now consider the photochemical case. For short burning times t_{off}, when the triplet bottle neck effect has not yet been fully established, the hole remains narrower (curve c) than for the corresponding closed three-level system. For increasing burning times the photochemical hole width becomes larger (curve d) than the steady-state width for this closed system. The behavior of the relative hole depth D for the cases just discussed, is shown in Fig. 7.

We now consider the question which extrapolation method should be used to obtain T_2 from a series of experimental hole widths. When $\Delta\nu^h$ is measured as a function of the burning time t_{off}, it can be seen from Fig. 5 (a) that for $\chi^2 = 2.97 \times 10^9$ s^{-2} the straight extrapolation to $t_{off} = 0$ would yield $\Delta\nu^h/2 > 1/\pi T_2$. Thus by just measuring $\Delta\nu^h$ as a function of t_{off} for a certain value of
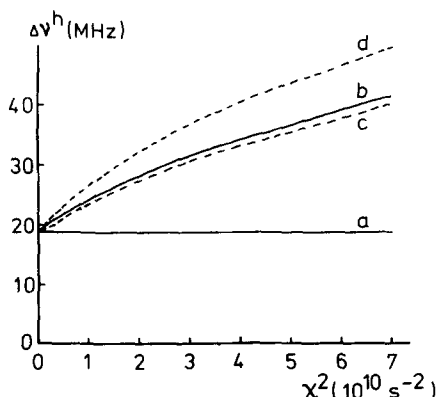

FIG. 6. Hole width (FWHM) as a function of χ^2 using the parameter values for porphin in n-octane at low temperature $(T_2 = 2\tau_{t1})$. The behaviour of the corresponding closed two-level (a) and three-level (b) systems as well as that of the photochemical case of Fig. 3 for burning times $t_{off} = 0.1$ s (c) and $t_{off} = 1$ s (d) is shown.
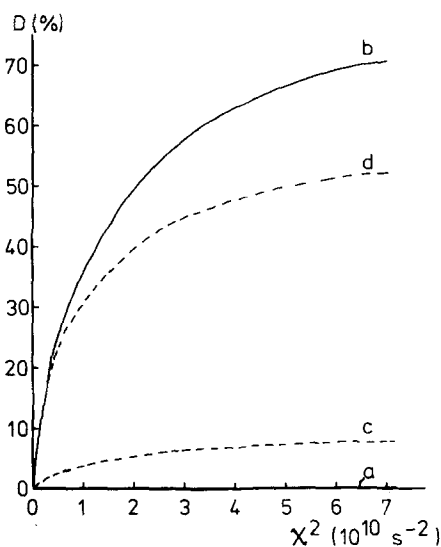

FIG. 7. Relative hole depth as a function of χ^2 using the parameter values for porphin in n-octane at low temperature $(T_2 = 2\tau_{t1})$. The characters (a)–(d) denote the same cases as in Fig. 6.

χ^2 will be insufficient to obtain an accurate value of T_2. Now consider $\Delta\nu^h$ as a function of χ^2 with, for example, $t_{off} = 1$ s. We applied the method discussed in Sec. III [Eq. (22)] and plotted $\pi T_2(\Delta\nu^h)^2 - 2(\Delta\nu^h)$ as a function of χ^2. Indeed straight lines were obtained. For $T_2 = 2\tau_{t1}$ it passed through the origin. It thus turns out that for porphin the functional relationship between $\Delta\nu^h$ and χ^2 is similar to that for the closed three-level system [Eq. (20)] and this extrapolation method as a function of χ^2 will yield a reliable value of T_2. However, as the analytical formula connecting $\Delta\nu^h$ with χ^2 is unknown in this case, the power extrapolation will not give a value for μ_{12} or k_{23} as for the closed three-level system. Thus for porphin in n-octane and for the range of parameter values considered, a simple extrapolation method is obtained, compared to what will generally be the case according to the statement in Sec. I, paragraph four.

Summarizing, we can state that the simulation method based upon the microscopic theory as presented above, provides precise insight in the porphin hole burning process. Also for temperature dependent measurements this simulation method would yield T_2 (the region $T_2 < 2\tau_{t1}$). When at low temperature the burning conditions (χ^2, t_{off}) are determined (using the simulations, whereby the problem of the local field correction is overcome), at a higher temperature under the same conditions one just has to vary T_2 in the simulation until the experimentally observed $\Delta\nu^h$ is obtained.

Finally it should be noted that with a kinetic theory instead of using a density matrix treatment we obtained nearly the same results.[8] For D the results are identical, while $\Delta\nu^h$ for the highest burning power and longest burning time considered [Figs. 5(a) and 6] is less than 1 MHz narrower with the kinetic treatment.

B. Dimethyl-s-tetrazine in durene

The level scheme applicable to this system will appear to be more complex than that of Fig. 3. As a conse-
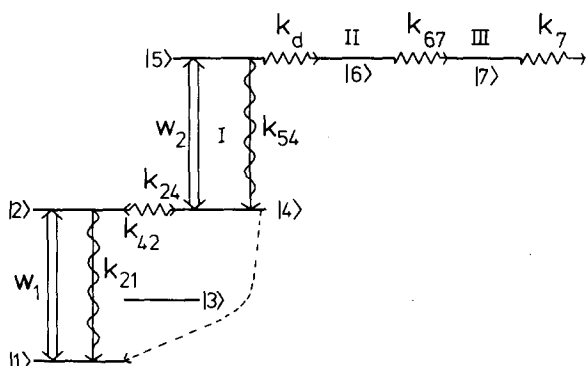
FIG. 8. Kinetic scheme chosen for DMST in durene at low temperature. The sawtooth arrows denote (possible) reactions to other chemical species (intermediates). The intermediates are denoted by Roman numbers. The scheme is further discussed in the text.

quence a kinetic treatment will be given instead of a density matrix theory like that of Sec. IV. Nevertheless the general approach of the DMST hole burning theory is similar to that of Sec. IV.

Our hole burning experiments on this system showed that at 1.8 K and for a 1 s burning time $\Delta\nu^h \approx 50$ MHz, which is completely determined by the 6 ns fluorescence lifetime.[1,9] We assumed a one-photon dissociation process. However, recent studies revealed[20,21] that this dissociation is accomplished by the sequential absorption of two photons. The question now arises how one can still experimentally find $\Delta\nu^h \approx 2/\pi T_2$. The answer will be given at the end of this subsection. The information recently obtained about this photodissociation process[20-22] shows that it is much more complicated then was originally assumed. Based upon this information we use the level scheme of Fig. 8 for the hole burning simulations. $|1\rangle$, $|2\rangle$, and $|3\rangle$ are the DMST S_0, S_1, and T states, respectively. Probably this is still a very simplified scheme. For instance, it is very well possible that level $|4\rangle$ is a vibronic level of some lower electronic state $|4'\rangle$ of intermediate I. The absorption of the second photon then would occur from $|4'\rangle$ after fast $|4'\rangle \rightarrow |4\rangle$ vibrational relaxation. Also $|4'\rangle$ might decay to its ground state $|4''\rangle$ which could have some probability of reacting back to ground state DMST. Such a possible pathway is indicated in Fig. 8 by the broken arrow. However, we will use the scheme of Fig. 8, where $|4\rangle$ directly absorbs the second photon, while it may also directly react back to $|2\rangle$. As we consider burning times, long compared to all inverse kinetic rates in the system, and take some value for the overall quantum yield of photodissociation independent of the level scheme considered, the simulations using the scheme of Fig. 8 will give quite realistic hole burning results. The population of the DMST triplet state $|3\rangle$ may be neglected.[72] Furthermore intermediate I will not give rise to the observed transient absorption spectrum,[21] as it absorbs at 5875 Å. Moreover I will dissociate faster than in 100 ns, otherwise its absorption would have been detected in the transient spectrum. But the intermediate giving the transient spectrum has a build-up time of ~6 μs.[22] This latter intermediate is

denoted by III in Fig. 8. The reasons why we chose the scheme of Fig. 8 will now be clear.

We now have to write down the equations of motion for the system in the presence of the burning field. We will treat this problem kinetically instead of using the density matrix. In the latter case, in the Laplace transformation procedure one would have to solve an equation of degree 8, which might not yield stable solutions. We therefore prefer a kinetic treatment, yielding an equation of only degree 4. Moreover, from the results obtained for porphin with both methods, we expect either treatment to yield (nearly) identical results (in principle). In the kinetic theory we encounter the induced transition rates w_1 and w_2 for the $|1\rangle - |2\rangle$ and the $|4\rangle - |5\rangle$ transition, respectively. They can be written as[10]:

$$w_1 = \frac{T_2}{2}\chi^2 \frac{1}{T_2^2\Delta^2 + 1} \tag{31}$$

$$w_2 = \frac{T_2'}{2}\chi^2 \frac{1}{T_2'^2\Delta'^2 + 1} . \tag{32}$$

Formula (31) may be used for times $t \gg T_2$ and for monochromatic excitation ($\Delta\nu_{exc} \ll 1/\pi T_2$). Similar conditions hold for w_2. T_2' is defined as the decay time of the density matrix element ρ_{45}. $\Delta = \omega_B - \bar\omega_0$ is the detuning from the burning frequency of a homogeneous line center $\bar\omega_0$ in the $|1\rangle - |2\rangle$ transition while $\Delta' = \omega_B - \bar\omega_0'$ is the detuning of a homogeneous center $\bar\omega_0'$ in the $|4\rangle - |5\rangle$ transition. As already mentioned in the beginning of Sec. II, the inhomogeneous broadening for different transitions will in general be different. Therefore there may exist a complex relationship between Δ and Δ' (belonging to a certain DMST molecule and the intermediate I formed from it), or no distinct relationship at all. We will use expression (32) for w_2 and study the hole burning results for different values of the ratio Δ'/Δ. This seems the best we can do for the moment. In fact, when $1/\pi T_2' \gtrsim \Delta\nu_G$, which seems quite realistic for DMST and ST, for all molecules to be pumped from $|4\rangle$ to $|5\rangle$ this will occur with nearly identical rates. In that case the precise distribution of Δ'/Δ values or the precise value of the constant Δ'/Δ will be unimportant for the final result, as shown by the results below. We assume the $|1\rangle - |2\rangle$ and $|4\rangle - |5\rangle$ transitions to have identical transition dipole moments. Thus $\chi = \mu_{12}E_0/\hbar = \mu_{45}E_0/\hbar$, where E_0 is the absolute value of the burning electric field amplitude $\mathbf{E}_0$. Expression (31) does not contain the power broadening term ($T_2^2\chi^2/2$) in the denominator,[10] and the same is true for expression (32). For the known value of T_2, the estimated one for χ^2 and the assumed values of T_2', these power broadening terms are $\ll 1$.

The equations of motion are:

$$\dot{N}_1 = w_1(N_2 - N_1) + k_{21}N_2 \tag{33}$$

$$\dot{N}_2 = w_1(N_1 - N_2) - K_2N_2 + k_{42}N_4 \tag{34}$$

$$\dot{N}_4 = w_2(N_5 - N_4) + k_{54}N_5 + k_{24}N_2 - k_{42}N_4 \tag{35}$$

$$\dot{N}_5 = w_2(N_4 - N_5) - K_5N_5 . \tag{36}$$

Here the total decay rate of $|2\rangle$ is $K_2 = k_{24} + k_{21}$, and that of $|5\rangle K_5 = k_d + k_{54}$ contains the rate (k_d) of loss of systems from the absorbing ensemble. N_1 denotes the population of level $|1\rangle$, etc. At the moment the burning starts ($t = 0$)

we have $N_1(0) = N$ and $N_2(0) = N_4(0) = N_5(0) = 0$. The time-dependent solution of these equations using the Laplace transformation technique proceeds in a similar way as the derivation given in the Appendix. In the present case only real solutions appear of the equation which is the analog of (A9). For the relative level population N_1/N, etc., sums of exponentials are obtained. At the moment the burning laser is shut off (t_{off}) we have the populations N_1/N (t_{off}, Δ), etc. After the decay of the excited states the DMST ground state population as a function of detuning is:

$$\frac{N_1}{N}(\Delta) = \left\{ \frac{N_1}{N}(t_{off}, \Delta) + \frac{N_2}{N}(t_{off}, \Delta) \right.$$
$$\left. + \frac{N_4}{N}(t_{off}, \Delta) + (1 - \emptyset_d)\frac{N_5}{N}(t_{off}, \Delta) \right\} , \quad (37)$$

where $\emptyset_d$ is the quantum yield from $|5\rangle$ for dissociation. Similar to the porphin case, we finally obtain for the probe absorption coefficient:

$$\alpha(:)\frac{1}{\pi T_2} \int_0^\infty \frac{N_1}{N}(\Delta)W\frac{1}{(\omega_p - \bar{\omega}_0)^2 + \frac{1}{T_2^2}} d\bar{\omega}_0 . \quad (38)$$

Assuming the probe laser to cause negligible population of levels $|2\rangle$ and further, one indeed measures the absorption line shape according to (38) (optically thin samples).

The numerical hole burning simulations using the theoretical results just given, were performed similarly as for the porphin case. For DMST this was done with the same resolution (2 MHz) but a larger region of integration (summation) was taken: from $+1$ to -1 GHz relative to ν_B. Plots were made of the ground state population hole [Eq. (37)] as well as of the hole in $\alpha(\nu_p)$.

For the kinetic parameters we have to make assumptions in agreement with the recent experimental observations.[20-22] First consider the lower transition. For the S_1 fluorescence lifetime $\tau_{f1} = 1/K_2$ we take 6 ns,[73] while in the low temperature limit $T_2 = 2\tau_{f1} = 2/K_2$.[10] For $S_0 - S_1$ a radiative lifetime was calculated of 4.5×10^{-7} s.[72] Assuming a certain amount of $S_0 - S_1$ internal conversion, we take $k_{21} = 5 \times 10^7$ s^{-1}. Further $k_{24} = K_2 - k_{21}$. Less information is available about the kinetic parameters of intermediate I. We suggest level $|5\rangle$ to be a vibronic level, exhibiting vibrational relaxation. The quantum yield from $|5\rangle$ for photodissociation will be high.[72,73] We assumed $\emptyset_d = 0.99$. As a consequence the dissociation rate k_d has to be high. For k_d a value of 10^{11} s^{-1} was taken, which still seems a low estimate. It is furthermore assumed that $k_{42} \ll k_{24}$: $k_{42} = 10^5$ s^{-1}. These assumptions yield $1/\pi T_2' = (K_5 + k_{42})/2\pi$ (low temperature limit[10]) $= 16.1$ GHz.

In Table I results of hole burning simulations are shown for several choices of the burning power (χ^2), the relative inhomogeneous distributions in the pumped transitions (Δ'/Δ) and the burning time t_{off}. It is shown that in the low power limit $\Delta\nu^h \approx 2/\pi T_2$. This is expected as $1/\pi T_2' \gg 1/\pi T_2$, and w_2 will be the same for all members of the frequency distribution pumped from $|1\rangle$ to $|2\rangle$. As another consequence these hole results are

TABLE I. DMST in durene at low temperature $(T_2 = 2\tau_{f1})$. Results of the simulations of the holes in the ground state population $N_1/N(\Delta)$ and in the absorption coefficient $\alpha(\nu_p)$ for the choices of the parameters indicated. The accuracy in the FWHM values is ± 0.3 MHz and in the D values $\pm 0.1\%$. For the inhomogeneous width of the $|1\rangle - |2\rangle$ transition was taken $\Delta\omega_G = 2\pi \times 7.3$ GHz.[1]

Parameters			Results		
			$N_1/N(\Delta)$	$\alpha(\nu_p)$	
χ^2(s^{-2})	Δ'/Δ	t_{off}(s)	FWHM(MHz)	FWHM(MHz)	$D(\%)$
10^{11}	1	1	26.2	51.9	0.7
10^{12}	1	1	37.9	61.8	41.2
10^{12}	10	1	38.4	61.3	41.1
5×10^{10}	1	1	26.2	~ 50	~ 0.2
10^{12}	1	2.5	53.6	75.8	65.0
10^{11}	1	25	29.4	54.4	15.0

nearly independent of Δ'/Δ, as shown. Note here that $\Delta'/\Delta = 10$ implies already a $|4\rangle - |5\rangle$ inhomogeneous width of ≥ 20 GHz. For larger values of k_d similar results are obtained. If $1/\pi T_2' < 1/\pi T_2$ was assumed, the low power result $\Delta\nu^h < 2/\pi T_2$ was obtained, and when $1/\pi T_2' \ll 1/\pi T_2$, this became $\Delta\nu^h \approx 1/\pi T_2$.

Estimating the pump rate from the purely radiative lifetime[72] and the experimental conditions, in our DMST hole burning experiments[1,9] we probably used values of χ^2 in the range $10^{12} - 10^{13}$ s^{-2}.

It is shown in this subsection that although the DMST photodissociation is a sequential two-photon process, it is very well possible to obtain for the hole in the absorption coefficient $\Delta\nu^h \approx 2/\pi T_2$. When more information will be obtained about the photodissociative mechanism, the method of simulation presented here can be used to obtain reliable T_2 values from accurate hole burning experiments.

C. s-Tetrazine in benzene

In our hole burning experiments on this system at 2 K we obtained a hole width (FWHM), extrapolated to zero burning time, of 0.7 ± 0.1 GHz.[9] From this width we calculated a fluorescence lifetime of 455 ps, where a one-photon dissociation was assumed. However, as for DMST, the dissociation of ST in benzene at low temperature was recently shown to have a sequential two-photon character.[20,21] Taking this into account, the theoretical results given below show that one may still obtain $\Delta\nu^h \approx 2/\pi T_2$.

Also for ST we will use the level scheme of Fig. 8. Again the population of the triplet state $|3\rangle$ can be neglected.[74] The kinetic theory and the numerical simulation program as used for DMST were applied for ST too. A resolution of 50 MHz was used in the present case, while the region of integration was taken from -17.5 to $+17.5$ GHz relative to ν_B.

For the kinetic parameters the following values were used. The S_1 fluorescence lifetime was taken to be $\tau_{f1} = 1/K_2 = 450$ ps,[75] while the low temperature limit was assumed: $T_2 = 2\tau_{f1}$.[10] For $S_0 - S_1$ a radiative lifetime was calculated of 4.0×10^{-7} s,[74] and a certain amount of S_0

TABLE II. ST in benzene at low temperature $(T_2 = 2\tau_{t1})$. Results of the simulations of the holes in the ground state population $N_1/N(\Delta)$ and in the absorption coefficient $\alpha(\nu_p)$ for the choices of the parameters indicated. The accuracy in the FWHM values is ±7 MHz and in the D values ±0.1%. For the inhomogeneous width of the $|1\rangle - |2\rangle$ transition was taken: $\Delta\omega_G = 2\pi \times 24.2$ GHz.[9]

Parameters		Results		
		$N_1/N(\Delta)$		$\alpha(\nu_p)$
Δ'/Δ	t_{off}(s)	FWHM(MHz)	FWHM(MHz)	$D(\%)$
1	1	515	≤876	12.4
10	1	475	≤764	11.9
10	5	590	876	44.1
10	10	735	988	62.9

~ S_1 internal conversion is admitted: $k_{21} = 5 \times 10^7$ s^{-1}. Further $k_{24} = K_2 - k_{21}$. About what happens after the $|4\rangle \leftarrow |2\rangle$ transition, for ST still less is known as for DMST. We took $k_{42} = 10^3$ s^{-1} and $\emptyset_d = k_d/K_5 = 0.99$.[72,73] Again k_d is assumed to be high (10^{11} s^{-1}) to make the competition with the $|4\rangle \leftarrow |5\rangle$ vibrational relaxation possible. As in the case of DMST we obtain $1/\pi T'_2 = 16.1$ GHz which again is $\gg 1/\pi T_2$. In the ST experiments[9] we probably used values of χ^2 in the region of 10^{11}–10^{12} s^{-2}, estimated from the purely radiative lifetime[74] and the experimental conditions.

In Table II the results of the simulations are shown for $\chi^2 = 5 \times 10^{10}$ s^{-2}. In the low power limit $\Delta\nu^h \approx 2/\pi T_2$ is obtainable, as expected, since $1/\pi T'_2 \gg 1/\pi T_2$. Assuming $1/\pi T'_2 \ll 1/\pi T_2$ yields $\Delta\nu^h \approx 1/\pi T_2$ for low power. From Tables I and II one can see that often the difference between the FWHM values of the holes in $N_1/N(\Delta)$ and in $\alpha(\nu_p)$ is less than $1/\pi T_2$, indicating the non-Lorentzian shape of the hole in the population $N_1/N(\Delta)$. The results of Table II show very good agreement with the experimentally obtained hole widths: With an experimental burning time of 5 s we obtained $\Delta\nu^h = 0.8 \pm 0.1$ GHz and for 10 s: 0.95 ± 0.1 GHz. We finally note here that our simulations show, that for $k_d \gtrsim 10^{12}$ s^{-1} no agreement with the experimental ST results can be obtained.

VI. CONCLUSIONS

In this paper we consider several types of hole burning theoretically and show how these methods may be utilized to obtain the homogeneous widths of optical transitions that are predominantly inhomogeneously broadened. We are especially interested in electronic transitions of guest molecules in low temperature organic mixed crystals. The theories are developed for simple model systems of singlet and triplet states. For the cases of two-level saturation and triplet bottle neck hole burning steady-state treatments are given. The holes so obtained are temporary. It is known that using these types of hole burning, the same information may be obtained as by the coherent transient method of OFID. Photochemical (and related photophysical) hole burning may lead, however, to *permanent* holes. Theoretical descriptions of this method are more complicated: A time-dependent treatment is necessary as molecules disappear from the ensemble under consideration.

We first considered a density matrix theory for two-level systems where the lower level is the ground state. The results agree with those obtained from gas phase two-level theories where both levels can decay to lower ones (more precisely with the so-called incoherent part of these results).

For the population bottle neck hole burning a three-level density matrix treatment was given for the first time, although this is closely related to molecular OFID theory.[18] A linear extrapolation method was discussed to obtain T_2 from such hole burning experiments. This power extrapolation may yield values for the transition dipole moment μ_{12} or the ISC rate k_{23}, as is the case for molecular OFID.[10,18] The Weisskopf–Heitler effect was argued to have no consequences for the feasibility of these experiments.

Next photochemical hole burning was considered, where the photoprocess is irreversible during the experiment (but the reaction may be forced in the opposite direction by radiation of another wavelength). Microscopic theories describing this process were not given before. We first treated the example of porphin in n-octane using equations of motion for the density matrix elements. These were solved time dependently with the Laplace transformation technique. The experimental results of Völker *et al.*[19] were simulated numerically and good agreement was obtained. For the porphin case we calculated the contributions to the observed hole width of the different types of hole burning discussed in this paper (Fig. 6). Linear extrapolation methods were considered, to obtain T_2 from porphin hole burning experiments.

Photochemical hole burning applied to DMST in durene was treated next kinetically. Here the situation is more complicated as the dissociation was recently found to be a sequential two-photon process. We present numerical simulation results using several assumptions concerning the kinetic parameters whose values are unknown at the moment. It is shown that, despite the two-photon character of the dissociation, it is very well possible to obtain an absorption hole width $\Delta\nu^h \approx 2/\pi T_2$, as was experimentally observed by us.[1,9]

Finally photochemical hole burning of ST in benzene at low temperature was treated in a similar way as DMST in durene, as also ST under these conditions was recently shown to dissociate by the sequential absorption of two photons. For several combinations of the kinetic parameter values it was theoretically shown that $\Delta\nu^h \approx 2/\pi T_2$ can be obtained. For one of these combinations good agreement was obtained with the experimental results for burning times of 5 and 10 s.

Although further experimental study of the photodissociation process of the tetrazines is interesting in itself, for the precise interpretation of the photochemical hole burning results such studies are necessary.

As a last point we want to note that, although the interpretation of our experimental hole burning results[1,9] is less simple as originally assumed, these results still form strong evidence that with $\Delta\nu_{exc} \ll 1/\pi T_2$ the singlet S_1 state was prepared upon excitation from S_0.[10]

ACKNOWLEDGMENTS

APPENDIX

Here we will give the time-dependent solution of the density matrix equations of motion (23)–(27), applying to photochemical hole burning. At $t = 0$ we have the conditions $\rho_{11}(0) = 1$ and $\rho_{22}(0) = \rho_{33}(0) = \bar{\rho}_{12}(0) = \bar{\rho}_{21}(0) = 0$. Now the Laplace transformed equations of motion become:

$$s r_1 - 1 = k_{21} r_2 + k_{31} r_3 + \tfrac{1}{2} i \chi (r_{21} - r_{12}) \tag{A1}$$

$$s r_2 = -K_2 r_2 + \tfrac{1}{2} i \chi (r_{12} - r_{21}) \tag{A2}$$

$$s r_3 = k_{23} r_2 - k_{31} r_3 \tag{A3}$$

$$s r_{12} = (-\Gamma + i\Delta) r_{12} + \tfrac{1}{2} i \chi (r_2 - r_1) \tag{A4}$$

$$s r_{21} = (-\Gamma - i\Delta) r_{21} - \tfrac{1}{2} i \chi (r_2 - r_1) , \tag{A5}$$

where $r_1(s)$ is the Laplace transform of $\rho_{11}(t)$, etc. For r_1 we obtain the solution:

$$r_1 = \frac{(s + K_2)\{(s + \Gamma)^2 + \Delta^2\}(s + k_{31}) + \tfrac{1}{2} \chi^2 (s + \Gamma)(s + k_{31})}{f(s)} , \tag{A6}$$

where

$$f(s) = (s^2 + K_2 s)\{(s + \Gamma)^2 + \Delta^2\}(s + k_{31}) + \tfrac{1}{2}\chi^2(2s + K_2)$$
$$\times (s + \Gamma)(s + k_{31}) - \tfrac{1}{2}\chi^2(s + \Gamma)\{k_{21}(s + k_{31}) + k_{23}k_{31}\} . \tag{A7}$$

$f(s)$ is of the fifth degree in s. To make the inverse Laplace transformation feasible, we like to write r_1 in the following form:

$$r_1 = \sum_{i=1}^{5} \frac{c_i}{s - s_i} . \tag{A8}$$

s_1–s_5 are the roots of the equation

$$f(s) = 0 , \tag{A9}$$

while the coefficients c_1–c_5 are obtained using the theory of partial fractions.[76] For example,

$$c_1 = \left(\frac{(s + K_2)\{(s + \Gamma)^2 + \Delta^2\}(s + k_{31}) + \tfrac{1}{2}\chi^2(s + \Gamma)(s + k_{31})}{(s - s_2)(s - s_3)(s - s_4)(s - s_5)} \right)_{s = s_1}. \tag{A10}$$

As discussed in Sec. V A the porphin holes are simulated numerically using the present theory. In these calculations Eq. (A9) was solved using the procedure POLZEROS (available at the University of Groningen computer centre). It turned out that sometimes all five roots were real, but for slightly different conditions two roots could be complex and could be written as $s_{j,k} = a \pm ib$. As a consequence $c_{j,k} = f \pm ig$. This causes the results obtained for $\rho_{11}(t)$, $\rho_{22}(t)$, and $\rho_{33}(t)$ always to be real, as it should be. When s_1 through s_5 are real the solution for $\rho_{11}(t)$ is:

$$\rho_{11}(t) = \sum_{i=1}^{5} c_i e^{s_i t} . \tag{A11}$$

When, for example, s_2, s_3, c_2, and c_3 are complex, we obtain

$$\rho_{11}(t) = c_1 e^{s_1 t} + 2 e^{at}(f \cos bt - g \sin bt) + c_4 e^{s_4 t} + c_5 e^{s_5 t} . \tag{A12}$$

Equations (A1)–(A5) further yield:

$$r_2 = \frac{\tfrac{1}{2}\chi^2(s + \Gamma)(s + k_{31})}{f(s)} . \tag{A13}$$

When Eq. (A9) only has real roots, we obtain:

$$\rho_{22}(t) = \tfrac{1}{2}\chi^2(c_6 e^{s_1 t} + c_7 e^{s_2 t} + c_8 e^{s_3 t} + c_9 e^{s_4 t} + c_{10} e^{s_5 t}) , \tag{A14}$$

where

$$c_6 = \left(\frac{(s + \Gamma)(s + k_{31})}{(s - s_2)(s - s_3)(s - s_4)(s - s_5)} \right)_{s = s_1} , \tag{A15}$$

etc. When two roots s are complex the sum of two of the exponentials in Eq. (A14) is replaced as done in Eq. (A12). For $r_3(s)$ we get:

$$r_3 = \frac{\tfrac{1}{2}\chi^2 k_{23}(s + \Gamma)}{f(s)} . \tag{A16}$$

For real roots s:

$$\rho_{33}(t) = \tfrac{1}{2}\chi^2 k_{23}(c_{11} e^{s_1 t} + c_{12} e^{s_2 t} + c_{13} e^{s_3 t} + c_{14} e^{s_4 t} + c_{15} e^{s_5 t}) , \tag{A17}$$

where

$$c_{11} = \left(\frac{s + \Gamma}{(s - s_2)(s - s_3)(s - s_4)(s - s_5)} \right)_{s = s_1} , \tag{A18}$$

etc. For two complex roots s, Eq. (A17) changes as described earlier.

Note added in proof: In a recent paper by Burland and Haarer [IBM J. Res. Develop. **23**, 534 (1979)] on the photochemistry of DMST, a reaction scheme different from the one in Fig. 8 is proposed. They suggest that the observed transient absorption spectrum[21] is due to the intermediate that absorbs the second photon. This seems unlikely in view of the fact that the two-photon character of the photodissociation was exposed with 6 ns dye laser pulses, while the transient spectrum shows a risetime of $\simeq 6$ μs. Moreover this transient shows no absorption at 5875 Å, which makes this interpretation questionable. We therefore claim that the scheme proposed in Fig. 8 is closer to reality. In this context we further wish to note that our parameter choice $k_{42} = 10^5$ s^{-1} for DMST is only apparently in contradiction with the fact that 100 ns after optical excitation intermediate I is no longer observed in the transient absorption spectrum. The level scheme in Fig. 8 indeed applies only to photochemical hole burning experiments with burning times $\gg$ all inverse kinetic rates.

[1]H. de Vries and D. A. Wiersma, Phys. Rev. Lett. **36**, 91 (1976).

[2]B. M. Kharlamov, R. I. Personov, and L. A. Bykovskaya, Opt. Commun. **12**, 191 (1974).

[3]A. A. Gorokhovski, R. K. Kaarli, and L. A. Rebane, JETP Lett. **20**, 216 (1974).

[4]T. J. Aartsma and D. A. Wiersma, Phys. Rev. Lett. **36**, 1360 (1976).

[5]W. H. Hesselink and D. A. Wiersma, Chem. Phys. Lett. **56**, 227 (1978).

[6]H. de Vries, P. de Bree, and D. A. Wiersma, Chem. Phys. Lett. **52**, 399 (1977); **53**, 418(E) (1978).

[7]T. E. Orlowski and A. H. Zewail, J. Chem. Phys. **70**, 1390 (1979).

[8]D. A. Wiersma, Adv. Chem. Phys. (to be published).

[9]H. de Vries and D. A. Wiersma, Chem. Phys. Lett. **51**, 565 (1977).

[10]H. de Vries and D. A. Wiersma, J. Chem. Phys. **70**, 5807 (1979); Erratum **71**, 5389 (1979).

[11]N. Bloembergen, E. M. Purcell, and R. V. Pould, Phys. Rev. **73**, 679 (1948).

[12]W. R. Bennett, Jr., Phys. Rev. **126**, 580 (1962).

[13]G. Mourou, B. Drouin, and M. M. Denariez-Roberge, Opt. Commun. **8**, 56 (1973).

[14]A. Szabo, Phys. Rev. B **11**, 4512 (1975).

[15]T. Muramoto, S. Nakanishi, and T. Hashi, Opt. Commun. **21**, 139 (1977).

[16]M. L. Spaeth and W. R. Sooy, J. Chem. Phys. **48**, 2315 (1968).

[17]R. M. Shelby and R. M. Macfarlane, Chem. Phys. Lett. **64**, 545 (1979).

[18]H. de Vries and D. A. Wiersma, J. Chem. Phys. **69**, 897 (1978).

[19]S. Völker, R. M. Macfarlane, A. Z. Genack, H. P. Trommsdorff, and J. H. van der Waals, J. Chem. Phys. **67**, 1759 (1977).

[20]D. M. Burland, F. Carmona, and J. Pacansky, Chem. Phys. Lett. **56**, 221 (1978).

[21]D. M. Burland and F. Carmona, Mol. Cryst. Liq. Cryst. **50**, 279 (1979).

[22]B. Dellinger, M. A. Paczkowski, R. M. Hochstrasser, and A. B. Smith, III, J. Am. Chem. Soc. **100**, 3242 (1978).

[23]V. S. Letokhov, in *High-Resolution Laser Spectroscopy*, Topics in Applied Physics, Vol. 13, edited by K. Shimoda (Springer, Berlin, 1976), p. 95.

[24]K. Shimoda, in *High-Resolution Laser Spectroscopy*, Topics in Applied Physics, Vol. 13, edited by K. Shimoda (Springer, Berlin, 1976), p. 11.

[25]G. Mourou, IEEE J. Quantum Electron. **QE-11**, 1 (1975).

[26]G. Mourou and M. M. Denariez-Roberge, Can. J. Phys. **52**, 2357 (1974).

[27]T. Kushida and E. Takushi, Phys. Rev. B **12**, 824 (1975).

[28]T. B. Tamm and P. M. Saari, Chem. Phys. Lett. **30**, 219 (1975).

[29]R. G. Brewer, in *Frontiers in Laser Spectroscopy, Les Houches* 1975, edited by R. Balian, S. Haroche, and S. Liberman (North Holland, Amsterdam, 1977), Vol. I, P. 341.

[30]F. Bloch, Phys. Rev. **70**, 460 (1946).

[31]L. Allen and J. H. Eberly, *Optical Resonance and Two-Level Atoms* (Wiley, New York, 1975), Chap. 6.

[32]M. Sargent III and P. E. Toschek, Appl. Phys. **11**, 107 (1976).

[33]M. Sargent III, P. E. Toschek, and H. G. Danielmeyer, Appl. Phys. **11**, 55 (1976).

[34]S. Haroche and F. Hartmann, Phys. Rev. A **6**, 1280 (1972).

[35]E. V. Baklanov and V. P. Chebotaev, Sov. Phys. JETP **33**, 300 (1971).

[36]E. V. Baklanov and V. P. Chebotaev, Sov. Phys. JETP **34**, 490 (1972).

[37]V. Weisskopf, Ann. Phys. **9**, 23 (1931).

[38]W. Heitler, *The Quantum Theory of Radiation*, 3rd ed. (Oxford University, Cambridge, England, 1954), pp. 196–203.

[39]H. M. Gibbs and T. N. C. Venkatesan, Opt. Commun. **17**, 87 (1976).

[40]C. Cohen-Tannoudji, in *Frontiers in Laser Spectroscopy, Les Houches* 1975, edited by R. Balian, S. Haroche and S. Liberman (North Holland, Amsterdam, 1977), Vol. I, pp. 82–96.

[41]H. Walther, in *Frontiers in Laser Spectroscopy, Les Houches* 1975, edited by R. Balian, S. Haroche, and S. Liberman (North Holland, Amsterdam, 1977), Vol. I, p. 125.

[42]W. H. Hesselink and D. A. Wiersma, Chem. Phys. Lett. **50**, 51 (1977).

[43]J. B. W. Morsink, W. H. Hesselink, and D. A. Wiersma, Chem. Phys. Lett. **64**, 1 (1979).

[44]B. di Bartolo, *Optical Interactions in Solids* (Wiley, New York, 1968), pp. 431–442.

[45]A. Z. Genack, R. M. Macfarlane, and R. G. Brewer, Phys. Rev. Lett. **37**, 1078 (1976).

[46]R. G. DeVoe, A. Szabo, S. C. Rand, and R. G. Brewer, Phys. Rev. Lett. **42**, 1560 (1979).

[47]L. E. Erickson, Opt. Commun. **21**, 147 (1977).

[48]L. E. Erickson, Phys. Rev. B **16**, 4731 (1977).

[49]R. M. Shelby and R. M. Macfarlane, Opt. Commun. **27**, 399 (1978).

[50]T. W. Hänsch, I. S. Shahin, and A. L. Schawlow, Phys. Rev. Lett. **27**, 707 (1971).

[51]R. A. Avarmaa and K. Kh. Mauring, Opt. Spectrosc. **41**, 393 (1976).

[52]R. M. Macfarlane and R. M. Shelby, Phys. Rev. Lett. **42**, 788 (1979).

[53]S. Völker, R. M. Macfarlane, and J. H. van der Waals, Chem. Phys. Lett. **53**, 8 (1978).

[54]B. M. Kharlamov, R. I. Personov, and L. A. Bykovskaya, Opt. Spectrosc. **39**, 137 (1975).

[55]A. A. Gorokhovski and J. Kikas, Zh. prikl. spektr. **28**, 832 (1978).

[56]W. H. Hesselink and D. A. Wiersma, Chem. Phys. Lett. **65**, 300 (1979).

[57]R. M. Hochstrasser and C. A. Nyi, J. Chem. Phys. **70**, 1112 (1979).

[58]A. A. Gorokhovski, R. Kaarli, and L. A. Rebane, Opt. Commun. **16**, 282 (1976).

[59]S. Völker and J. H. van der Waals, Mol. Phys. **32**, 1703 (1976).

[60]A. A. Gorokhovski and L. A. Rebane, Opt. Commun. **20**, 144 (1977).

[61]A. A. Gorokhovski and J. Kikas, Opt. Commun. **21**, 272 (1977).

[62]S. Volker and R. M. Macfarlane, Chem. Phys. Lett. **61**, 421 (1979).

[63]A. P. Marchetti, M. Scozzafava, and R. H. Young, Chem. Phys. Lett. **51**, 424 (1977).

[64]F. Graf, H.-K. Hong, A. Nazzal, and D. Haarer, Chem. Phys. Lett. **59**, 217 (1978).

[65]J. M. Hayes and G. J. Small, Chem. Phys. **27**, 151 (1978).

[66]J. M. Hayes and G. J. Small, Chem. Phys. Lett. **54**, 435 (1978).

[67]S. L. Hager and J. E. Willard, J. Chem. Phys. **61**, 3244 (1974).

[68]M. Dubs and Hs. H. Günthard, Chem. Phys. Lett. **64**, 105 (1979).

[69]Laser Focus **14** (9), 30 (1978).

[70]W. G. van Dorp, W. H. Schoemaker, M. Soma, and J. H. van der Waals, Mol. Phys. **30**, 1701 (1975).

[71]A. T. Gradyushko and M. P. Tsvirko, Opt. Spectrosc. **31**, 291 (1971).

[72]R. M. Hochstrasser, D. S. King, and A. B. Smith, III, J. Am. Chem. Soc. **99**, 3923 (1977).

[73]J. H. Meyling, R. P. van der Werf, and D. A. Wiersma, Chem. Phys. Lett. **28**, 364 (1974).

[74]R. M. Hochstrasser and D. S. King, J. Am. Chem. Soc. **98**, 5443 (1976).

[75]R. M. Hochstrasser, D. S. King, and A. C. Nelson, Chem. Phys. Lett. **42**, 8 (1976).

[76]*Handbook of Chemistry and Physics*, 47th ed. (Chemical Rubber, Cleveland, 1966), p. A236.